

Staleness-Alleviated Distributed GNN Training via Online Dynamic-Embedding Prediction

Guangji Bai^{1*}, Ziyang Yu^{2*}, Zheng Chai³, Yue Cheng³, Liang Zhao^{1†}

¹Emory University, ²University of Waterloo, ³University of Virginia

Abstract

Despite the recent success of Graph Neural Networks (GNNs), it remains challenging to train GNNs on large-scale graphs due to neighbor explosions. As a remedy, distributed computing becomes a promising solution by leveraging abundant computing resources (e.g., GPU). However, the node dependency of graph data increases the difficulty of achieving high concurrency in distributed GNN training, which suffers from the massive communication overhead. To address it, *Historical value approximation* is deemed a promising class of distributed training techniques. It utilizes an offline memory to cache historical information (e.g., node embedding) as an affordable approximation of the exact value and achieves high concurrency. However, such benefits come at the cost of involving dated training information, leading to staleness, imprecision, and convergence issues. To overcome these challenges, this paper proposes SAT (Staleness-Alleviated Training), a novel and scalable distributed GNN training framework that reduces the embedding staleness adaptively. The key idea of SAT is to model the GNN’s embedding evolution as a temporal graph and build a model upon it to predict future embedding, which effectively alleviates the staleness of the cached historical embedding. We propose an online algorithm to train the embedding predictor and the distributed GNN alternatively and further provide a convergence analysis. Empirically, we demonstrate that SAT can effectively reduce embedding staleness and thus achieve better performance and convergence speed on multiple large-scale graph datasets.

Introduction

Graph Neural Networks (GNNs) have shown impressive success in analyzing non-Euclidean graph data and have achieved promising results in various applications, including social networks, recommender systems, and knowledge graphs, etc. (Dai, Dai, and Song 2016; Ying et al. 2018; Lei et al. 2019; Ling et al. 2022). Despite their great promise, GNNs meet significant challenges when being applied to large graphs, which are common in the real world—the number of nodes goes beyond millions or even billions. Training GNNs on large graphs is jointly challenged by the lack of inherent parallelism in the backpropagation optimization and

heavy inter-dependencies among graph nodes, rendering existing parallel techniques inefficient. To tackle such unique challenges, distributed GNN training is a promising open domain that has attracted fast-increasing attention in recent years and has become the *de facto* standard for fast and accurate training over large graphs (Thorpe et al. 2021; Ramezani et al. 2021; Wan et al. 2022b; Chai et al. 2022).

A key challenge in distributed GNN training lies in obtaining accurate node embeddings based on the neighbor nodes and subgraphs while avoiding massive communication overhead incurred by the message passing across them. On the one hand, naively partitioning the graph into different subgraphs by dropping the edges across them can reduce communications among subgraphs. However, this will result in severe information loss and highly inaccurate approximation of node embeddings (Angerd, Balasubramanian, and Annaram 2020; Jia et al. 2020; Ramezani et al. 2021). On the other hand, propagating all the information between different subgraphs will guarantee accurate node embeddings, while inevitably suffering huge communication overhead and plagued efficiency due to neighbor explosion (Ma et al. 2019; Zhu et al. 2019; Zheng et al. 2020; Tripathy, Yelick, and Buluç 2020). More recently, using historical value to approximate the exact one has been widely used and achieved SOTA performance in large-scale GNN training (Fey et al. 2021; Wan et al. 2022b; Yu et al. 2022; Chai et al. 2022). Specifically, by leveraging an offline memory to cache *historical embeddings* (e.g., of the nodes) to approximate true embeddings, such methods can achieve a constant communication cost over graph size while the inter-dependency between subgraphs is retained.

However, the aforementioned idea is bottlenecked by the *staleness* of the historical embeddings. Such dated embeddings further lead to staleness and imprecision in the gradients of the embeddings and model parameters during the backward pass. As shown in Figure 1, we measure the staleness of historical embeddings (red curves) of a GCN trained on 2 graph datasets, and the staleness error is nontrivial throughout the entire training. The staleness error degrades the model’s performance and slows the convergence, which we empirically validated in our experiment section.

Alleviating the staleness means making the historical embedding a more accurate and timely estimate of the actual embedding, which is, though appealing, difficult to achieve

*These authors contributed equally.

†Corresponding Author

Under review. Do NOT distribute.

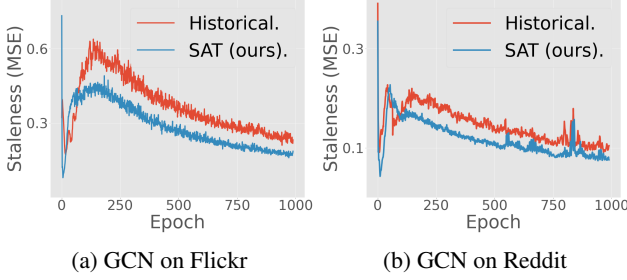


Figure 1: **Embedding staleness and its alleviation.** Comparison of embedding staleness with (blue) or without (red) our method. The staleness error is measured with respect to the full-graph training’s embedding which has zero staleness.

due to several challenges: **1). Difficulties in tracking the dynamics of the true embeddings.** Alleviating the staleness requires not only modeling the temporal patterns and trends of actual and historical embeddings across iterations but also capturing these embeddings’ mutual dependencies used in GNN computation; **2). Difficulty in designing an efficient and scalable algorithm for staleness reduction.** Adjusting the historical embedding incurs extra computational overhead. So it is challenging to ensure a better trade-off between its cost and quality toward a substantial performance gain. **3). Unknown impact on the model training.** Using the adjusted historical embedding may change the properties of the training process of GNNs and trouble its convergence and stability. Theoretical analysis and guarantee are imperative yet nontrivial due to the involvement of historical adjustment.

Our Contribution. To jointly address all challenges above, we propose a novel distributed GNN training framework toward an appealing trade-off between concurrency and quality of embedding calculation with Staleness Alleviation Training, or SAT. In SAT, we design a new architecture called the *embedding predictor* that handles the staleness issue in a data-driven manner and enjoys good scalability. We innovatively formulate the distributed GNN’s embeddings as a sequence of *temporal graphs* with their nodes & edges induced by the original graph and the time defined as training epochs, where each temporal graph fully characterizes the evolution of node embeddings for each local GNN. Based on the temporal graphs, we further propose a multi-task learning loss to jointly optimize the embedding predictor and the temporal graphs, where each task corresponds to the embedding prediction on a specific local subgraph. In terms of the optimization of SAT framework, due to the fact that the parameters of the distributed GNN and the embedding predictor are *coupled* and form a nested optimization problem, we propose an online algorithm to train each model alternatively and provide the theoretical guarantees of how the embedding predictor could affect the convergence under the distributed setting. Finally, we perform extensive evaluations over 6 comparison methods on 8 real-world graph benchmarks with 2 different GNN operators, where our framework can boost existing state-of-the-art methods’ performance and convergence speed by a great margin as a result of reduced staleness in node embeddings.

Preliminaries and Related Work

Graph Neural Networks. GNNs aim to learn a function of signals/features on a graph $\mathcal{G}(\mathcal{V}, \mathcal{E})$ with node embeddings $\mathbf{X} \in \mathbb{R}^{|\mathcal{V}| \times d}$, where d denotes the node feature dimension. For typical semi-supervised node classification tasks (Kipf and Welling 2016), where each node $v \in \mathcal{V}$ is associated with a label \mathbf{y}_v , a L -layer GNN \mathbf{f}_θ parameterized by θ is trained to learn the node embedding \mathbf{h}_v such that \mathbf{y}_v can be predicted accurately. Analytically, the ℓ -th layer of the GNN is defined as

$$\begin{aligned} \mathbf{h}_v^{(\ell+1)} &= \mathbf{f}_\theta^{(\ell+1)}\left(\mathbf{h}_v^{(\ell)}, \{\{\mathbf{h}_u^{(\ell)}\}_{u \in \mathcal{N}(v)}\}\right) \\ &= \Psi_\theta^{(\ell+1)}\left(\mathbf{h}_v^{(\ell)}, \Phi_\theta^{(\ell+1)}\left(\{\{\mathbf{h}_u^{(\ell)}\}_{u \in \mathcal{N}(v)}\}\right)\right), \end{aligned} \quad (1)$$

where $\mathbf{h}_v^{(\ell)}$ denotes the embedding of node v in the ℓ -th layer, and $\mathbf{h}_v^{(0)}$ being initialized to \mathbf{x}_v (v -th row in \mathbf{X}), and $\mathcal{N}(v)$ represents the set of neighborhoods for node v . Each layer of the GNN, i.e. $\mathbf{f}_\theta^{(\ell)}$, can be further decomposed into the aggregation function $\Phi_\theta^{(\ell)}$ and the updating function $\Psi_\theta^{(\ell)}$, and both functions can choose to use various functions in different types of GNNs.

Distributed Training for GNNs. Distributed GNN training first partitions the original graph into multiple subgraphs without overlap, which can also be considered mini-batches. Then different mini-batches are trained in different devices in parallel. Here, Eq. 1 can be further reformulated as

$$\begin{aligned} \mathbf{h}_v^{(\ell+1)} &= \mathbf{f}_\theta^{(\ell+1)}\left(\mathbf{h}_v^{(\ell)}, \underbrace{\{\{\mathbf{h}_u^{(\ell)}\}_{u \in \mathcal{N}(v) \cap \mathcal{S}(v)}\}}_{\text{In-subgraph nodes}} \right. \\ &\quad \left. \cup \underbrace{\{\{\mathbf{h}_u^{(\ell)}\}_{u \in \mathcal{N}(v) \setminus \mathcal{S}(v)}\}}_{\text{Out-of-subgraph nodes}}\right), \end{aligned} \quad (2)$$

where $\mathcal{S}(v)$ denotes the subgraph that node v belongs to. In this paper, we consider the distributed training of GNNs with multiple local machines and a global server. The original input graph \mathcal{G} is first partitioned into M subgraphs, where each $\mathcal{G}_m(\mathcal{V}_m, \mathcal{E}_m)$ represents the m -th subgraph. Our goal is to find the optimal parameter θ in a distributed manner by minimizing the global loss

$$\min_\theta \mathcal{L}_{\text{global}}(\theta) = \sum_{m=1}^M \mathbf{w}_m \cdot \mathcal{L}_{\text{local}}^{(m)}(\theta), \quad (3)$$

where \mathbf{w}_m denotes the averaging weights and for each local loss and the local losses are given by

$$\mathcal{L}_{\text{local}}^{(m)}(\theta) = \frac{1}{|\mathcal{V}_m|} \sum_{v \in \mathcal{V}_m} \text{Loss}(\mathbf{h}_v^{(L)}, \mathbf{y}_v), \quad \forall m. \quad (4)$$

Existing methods in distributed training for GNNs can be classified into two categories, namely “*partition-based*” and “*propagation-based*”. The “Partition-based” method (Angerd, Balasubramanian, and Annavaram 2020; Jia et al. 2020; Ramezani et al. 2021) generalizes the existing data parallelism techniques of classical distributed training on *i.i.d* data to graph data and enjoys minimal communication cost. However, the embeddings of neighbor nodes (“out-of-subgraph

nodes” in Eq. 2) is dropped and the connections between sub-graphs are thus ignored, which results in severe information loss. Hence, another line of work, namely the ”propagation-based” method (Ma et al. 2019; Zhu et al. 2019; Zheng et al. 2020; Tripathy, Yelick, and Buluç 2020; Wan et al. 2022b) considers using communication of neighbor nodes for each subgraph (”out-of-subgraph nodes” in Eq. 2) to satisfy GNN’s neighbor aggregation, which minimizes the information loss. However, due to the *neighborhood explosion* problem, inevitable communication overhead is incurred and plagues the achievable training efficiency.

GNNs with Historical Value Approximation. The idea of considering *historical values* (of embedding, gradient, etc) as an approximation of the exact values can date back to distributed training on *i.i.d* data (Huo et al. 2018; Xu, Huo, and Huang 2020). With the rising popularity of GNNs, such an idea has been extended to train GNNs, especially on large-scale graphs. For example, in sampling-based methods, VR-GCN (Chen, Zhu, and Song 2018) uses historical embeddings to reduce neighbor sampling variance. GNNAutoScale (Fey et al. 2021) leverages historical embeddings of *1-hop* neighbors to achieve efficient mini-batch training. GraphFM (Yu et al. 2022) applies a momentum step on historical embeddings to obtain better embedding approximations of sampled nodes. In distributed GNN training, PipeGCN (Wan et al. 2022b) proposed a pipeline parallelism training for GNNs based on historical embeddings and gradients. DIGEST (Chai et al. 2022) leverages historical embeddings to achieve computation-storage separation and partition-parallel training. A more comprehensive discussion of existing work and our proposed method can be found in the appendix.

Problem Formulation

We follow the partition-parallel distributed training of GNNs defined in Eq. 3. Given the m -th graph partition \mathcal{G}_m , we reformulate Eq. 2 in the matrix form as

$$\mathbf{H}_{in}^{(\ell+1,m)} = \mathbf{f}_{\theta_m}^{(\ell+1)} \left(\mathbf{H}_{in}^{(\ell,m)}, \mathbf{H}_{out}^{(\ell,m)} \right), \quad (5)$$

where $\mathbf{H}_{in}^{(\ell,m)}$ and $\mathbf{H}_{out}^{(\ell,m)}$ denotes the in- and out-of-subgraph node embeddings at ℓ -th layer on partition \mathcal{G}_m , respectively. As mentioned earlier, directly swapping $\mathbf{H}_{out}^{(\ell,m)}$ between each subgraph will result in exponential communication costs and harm the concurrency of distributed training. Existing historical-value-based methods approximate the out-of-subgraph embeddings by historical embeddings $\tilde{\mathbf{H}}_{out}^{(\ell,m)}$, which result in a staleness error, i.e.,

$$\delta \tilde{\mathbf{H}}^{(\ell,m)} := \left\| \mathbf{H}_{out}^{(\ell,m)} - \tilde{\mathbf{H}}_{out}^{(\ell,m)} \right\|. \quad (6)$$

In this work, we consider predicting $\mathbf{H}_{out}^{(\ell,m)}$ in an efficient and data-driven manner such that the predicted embedding $\hat{\mathbf{H}}_{out}^{(\ell,m)}$ has a smaller staleness than $\tilde{\mathbf{H}}_{out}^{(\ell,m)}$. Despite the necessity, how to handle the above problem is an open research area due to several existing challenges: 1). The underlying evolution of the true embedding $\mathbf{H}_{out}^{(\ell,m)}$ is unknown and complicated due to the nature of GNN’s computation and distributed training; 2). How to design the algorithm to reduce

the staleness without hurting the efficiency and scalability of distributed training is highly non-trivial. 3). How the added staleness alleviation strategies will impact the model training process, such as the convergence and stability, is difficult yet important question to address.

Proposed Method

This section introduces our framework Staleness-Alleviated Training (SAT) that jointly addresses the challenges above. We first present an overview of SAT, followed by introducing our proposed embedding predictor, a novel architecture that adaptively captures the evolution of node embeddings with specially designed input data and training objectives. Finally, we demonstrate the proposed online algorithm for optimizing the framework with a theoretical convergence guarantee.

Overview of SAT

Figure 2 provides the detailed end-to-end flow of SAT, where the embedding predictor reduces the staleness of historical embeddings by leveraging their evolution pattern over past epochs. This is achieved by modeling distributed GNN’s embeddings as *temporal graphs* such that the embedding predictor jointly captures the spatial and temporal evolution. The predicted embeddings serve as a better approximation of ground truth and are pulled by each machine as additional inputs in their parallel forward propagation, which can be expressed as

$$\mathbf{H}_{in}^{(\ell+1,m)} \approx \mathbf{f}_{\theta_m}^{(\ell+1)} \left(\mathbf{H}_{in}^{(\ell,m)}, \underbrace{\mathbf{g}_{\omega}(\mathcal{G}_{tmp}^{(m)})}_{\text{Predicted embeddings}} \right), \quad (7)$$

where $\mathbf{g}_{\omega}(\cdot)$ denotes the embedding predictor, and $\mathcal{G}_{tmp}^{(m)}$ represents the temporal graph for the m -th partition. Note that the pulled predicted embeddings are only for out-of-subgraph nodes hence the communication cost is kept low. The entire framework can be trained via an online algorithm.

Embedding Predictor

Here we introduce our proposed embedding predictor $\mathbf{g}_{\omega}(\cdot)$ which aims to alleviate the staleness error defined in Eq. 6. Our contribution is 2-fold: First, we innovatively formulate the embedding prediction task as modeling the temporal graphs induced by the distributed GNN over different epochs. The temporal graphs fully characterize the underlying evolution of node embeddings, thus enabling our predictor to predict the target embeddings with sufficient information. Second, to jointly optimize the embedding predictor and the induced temporal graphs, we propose a new multi-task learning loss where each task corresponds to the embedding prediction on each graph partition.

Temporal Graphs Induced by Distributed GNNs. Recall the forward propagation of distributed GNN defined in Eq. 5, our goal is to predict the out-of-subgraph embeddings for the current training epoch such that the predicted embeddings offer a better approximation than historical embeddings. Intuitively, every local GNN computes the node embeddings in a recursive way by message passing across multiple layers, while the usage of historical embeddings further introduces

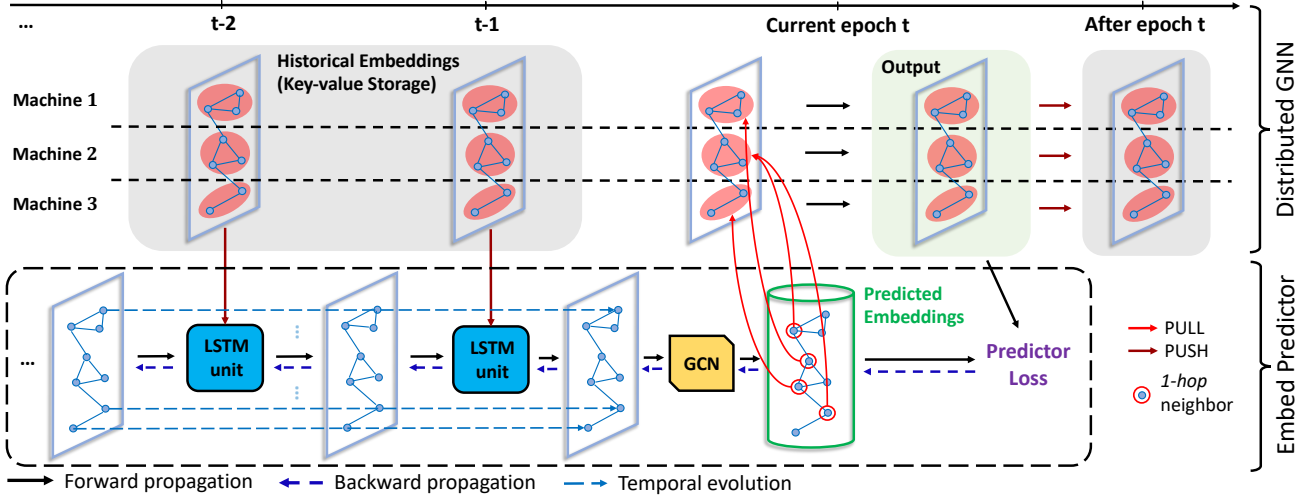


Figure 2: **Overview of our proposed SAT framework** (per-GNN-layer view). The upper body depicts the parallel distributed training of the GNN, and the lower body depicts that our embedding predictor reduces the embedding staleness by modeling how embeddings evolve temporally and spatially. The predicted embeddings are pulled to each machine for highly concurrent training of the GNN, and its output during the forward pass serves as weak supervision to train the embedding predictor. Such a design decouples the computation of these two components and allows us to train them in an efficient online manner. Our proposed embedding predictor is general and method-agnostic, i.e., holding the potential for enhancing the quality and relevance of historical embeddings, which could lead to improvements in various applications and domains.

the previous epoch’s information. Hence, our goal requires the proposed embedding predictor to jointly capture the spatial (*across-layer*) and temporal (*across-epoch*) evolution of the node embeddings.

To this end, we need to define the input data for the embedding predictor such that the data sufficiently characterize the underlying evolution of embeddings. To see this, consider the subgraph $\bar{\mathcal{G}}_m = (\bar{\mathcal{V}}_m, \bar{\mathcal{E}}_m)$ induced by the m -th graph partition \mathcal{G}_m and its 1-hop neighborhoods, where the edges between them are preserved as in the original raw graph. Denote the in- and out-of-subgraph embeddings computed by the local GNN model at epoch t as $\mathbf{H}_{in}^{(t,\ell,m)}$ and $\mathbf{H}_{out}^{(t,\ell,m)}$, where ℓ goes from 1 to L . The key observation here is that if we plug these node embeddings into $\bar{\mathcal{G}}_m$ as node weights, we can actually define a *temporal graph* $\{\bar{\mathcal{G}}_m^{(t)}\}_{t \in \mathcal{T}}$ as

$$\{\bar{\mathcal{G}}_m^{(t)}\}_{t \in \mathcal{T}} := \left\{ \left(\bar{\mathcal{V}}_m, \bar{\mathcal{E}}_m, \{\mathbf{H}_{in}^{(t,\ell,m)}\}_{\ell=1}^L, \{\mathbf{H}_{out}^{(t,\ell,m)}\}_{\ell=1}^L \right) : t = 1, 2, \dots, T \right\}, \quad (8)$$

where T denotes the total number of epochs. In temporal graph $\{\bar{\mathcal{G}}_m^{(t)}\}_{t \in \mathcal{T}}$, each node and edge is the same as in the original full graph, and the timestamp t is defined as each training epoch. Based on Eq. 8, the entire set of temporal graphs induced by the distributed GNN can be defined as $\{\bar{\mathcal{G}}^{(t)}\}_{t \in \mathcal{T}} := \{\{\bar{\mathcal{G}}_m^{(t)}\}_{m=1}^M : t = 1, 2, \dots, T\}$, where M denotes the number of subgraphs.

Multi-task Learning of Embedding Predictor. Given the temporal graph defined above, our *goal* is to build an embedding predictor that proactively captures the evolving pattern and predicts embeddings for the current epoch. The key observation here is that each subgraph induces a temporal graph

and we want to jointly train an embedding predictor that is able to make predictions for any subgraphs. Multi-task Learning (MTL (Zhang and Yang 2021)), which jointly trains a model on multiple different tasks to improve the generalization ability, provides a suitable option for our problem. Formally, to learn the embedding predictor g_ω parameterized by ω we optimize the following objective at epoch t :

$$\min_{\omega_t} \frac{1}{M} \sum_{m=1}^M \left\| g_{\omega_t}(\{\bar{\mathcal{G}}_m^{(s)}\}_{t-\tau \leq s \leq t-1}) - \mathbf{H}^{(t,m)} \right\|, \quad (9)$$

s.t., $\delta \hat{\mathbf{H}}^{(t,m)} < \delta \mathbf{H}^{(t-1,m)}, \forall m,$

where $\mathbf{H}^{(t,m)}$ denotes the concatenation of in- and out-of-subgraph embeddings without any staleness, $\hat{\mathbf{H}}^{(t,m)}$ is a compact notation of the output by g_{ω_t} , and τ denotes the length of the *sliding window* where we restrain the mapping function can only access up to τ steps of historical information.

In this work, we consider combining GNNs with *recurrent structures* as embedding predictors. The GNN captures the information within the node dependencies while the recurrent structure captures the information within their temporal evolution. Specifically, we consider implementing our embedding predictor g_ω as an RNN-GNN (Wu et al. 2022). The combination of LSTM and GCN is what we found empirically the optimal trade-off between efficiency and capacity in most cases, while the RNN-GNN is generic for many different variants (LSTM-GAT, GRU-GCN, etc.)

Optimization Algorithm

Here we demonstrate the general loss function of SAT and the proposed optimization algorithm. The detailed algorithm is shown in Algorithm 1. With the additional embedding

predictor, the training procedure for SAT is more complicated than standard distributed GNN training. As a result, jointly optimizing the GNN and embedding predictor is tricky due to the fact that the forward passes of the two models are *coupled*. To see this, the overall loss of SAT can be expressed as a *nested* optimization as follows

$$\begin{aligned} \forall m, \theta_m^* &= \arg \min_{\theta_m} \mathcal{L}_{\text{local}}^{(m)}(\theta_m, \omega_t^*), \\ \text{s.t., } \omega_t^* &= \arg \min_{\omega_t} \mathcal{L}_{\text{Pred}}(\omega_t, \{\theta_m^*\}_{m=1}^M). \end{aligned} \quad (10)$$

By following Eq. 3 and plugging our embedding predictor into Eq. 2, the distributed GNN's loss is

$$\mathcal{L}_{\text{local}}^{(m)}(\theta_m, \omega_t^*) = \frac{1}{|\mathcal{V}_m|} \sum_{v \in \mathcal{V}_m} \text{Loss}(\mathbf{h}_v^{(L)}, \mathbf{y}_v), \quad (11)$$

where it recursively satisfies

$$\begin{aligned} \mathbf{h}_v^{(L)} &= \mathbf{f}_{\theta_m}^{(L)} \left(\left\{ \left\{ \mathbf{h}_u^{(L-1)} \right\}_{u \in \mathcal{N}(v) \cap \mathcal{S}(v)} \right\} \right. \\ &\quad \left. \left\{ \left\{ \mathbf{g}_{\omega_t^*}^{(s)} \left(\{\bar{\mathcal{G}}_m^{(s)}\}_{t-\tau \leq s \leq t-1} \right) \right\}_{u \in \mathcal{N}(v) \setminus \mathcal{S}(v)} \right\}^{L-1} \right). \end{aligned} \quad (12)$$

By plugging the distributed GNN's forward pass into Eq. 15, the embedding predictor's loss is

$$\begin{aligned} \mathcal{L}_{\text{Pred}}(\omega_t, \{\theta_m^*\}) &= \frac{1}{M} \sum_m \left\| \mathbf{g}_{\omega_t} \left(\{\bar{\mathcal{G}}_m^{(s)}\}_{t-\tau \leq s \leq t-1} \right) - \right. \\ &\quad \left. \left\{ \mathbf{f}_{\theta_m^*}^{(\ell+1)}(\mathbf{H}_{\text{in}}^{(t,\ell,m)}, \hat{\mathbf{H}}_{\text{out}}^{(t,\ell,m)}) \right\}_{\ell=0}^{L-1} \right\|. \end{aligned} \quad (13)$$

The key observation here is that the predicted embeddings $\mathbf{g}_{\omega_t}(\{\bar{\mathcal{G}}_m^{(s)}\}_{t-\tau \leq s \leq t-1})$ have a 2-fold functionality: 1) it serves as an additional input in the forward propagation of the distributed GNN, and 2) it serves as the prediction to calculate the loss function of the embedding predictor. Noticing this, we propose an online algorithm to train the GNN model and the embedding predictor *alternatively*, which decouples the 2-fold functionality and allows easier optimization. The pseudo-code for SAT's training procedure is provided in Algorithm 1, and a more detailed optimization process of our online algorithm can be found in the appendix.

Theoretical Analyses

Convergence Analyses. Here we analyze the convergence of SAT. We show that the global GNN model can converge under the distributed training setting with the embedding predictor. Due to limited space, more details such as the proof can be found in the appendix.

Theorem 0.1. *Consider a GCN with L layers that are L_f -Lipschitz smooth. $\forall \epsilon > 0, \exists$ constant $E > 0$ such that, we can choose a learning rate $\eta = \sqrt{M}\epsilon/E$ and number of training iterations $T = (\mathcal{L}(\theta^{(1)}) - \mathcal{L}(\theta^*))EM^{-\frac{1}{2}}\epsilon^{-\frac{3}{2}}$, s.t.,*

$$\frac{1}{T} \sum_{t=1}^T \left\| \nabla \mathcal{L}(\theta^{(t)}) \right\|_2^2 \leq \mathcal{O} \left(\frac{1}{T^{\frac{2}{3}} M^{\frac{1}{3}}} \right), \quad (14)$$

where θ^* denotes the optimal parameter for the global GCN.

Communication Cost Analyses. Here we analyze the communication cost of SAT as depicted in Algorithm 1. Without loss of generality, consider a GNN with L layers and a

Algorithm 1: Staleness-alleviated Distributed GNN Training

Require: GNN learning rate η_1 , embedding predictor learning rate η_2 , update frequency ΔT .

```

1: /* Partitioning the raw graph */
2:  $\{\mathcal{G}_m(\mathcal{V}_m, \mathcal{E}_m), m = 1, \dots, M\} \leftarrow \text{METIS}(\mathcal{G})$ 
3: for  $t = 1 \dots T$  do
4:   for  $m = 1 \dots M$  in parallel do
5:     for  $\ell = 1 \dots L$  do
6:       Pull  $\hat{\mathbf{H}}_{\text{out}}^{(\ell,m)}$  to local machines
7:       Forward prop for local GNNs as Eq. 7
8:       Push computed embeddings to the server
9:     end for
10:    /* Local GNN update */
11:    Compute local loss as Eq. 11 and gradients  $\nabla \theta_m^{(t)}$ 
12:     $\theta_m^{(t+1)} = \theta_m^{(t)} - \eta_1 \cdot \nabla \theta_m^{(t)}$ 
13:  end for
14:  /* Global GNN update */
15:   $\theta^{(t+1)} \leftarrow \text{AGG}(\theta_1^{(t+1)} \dots \theta_M^{(t+1)})$ 
16:  /* Embedding predictor update */
17:  if  $t \% \Delta T == 0$  then
18:    Compute embedding predictor loss as Eq. 13
19:     $\omega_{t+1} = \omega_t - \eta_2 \cdot \nabla \mathcal{L}_{\text{Pred}}(\omega_t)$ 
20:    Update predicted embeddings by  $\mathbf{g}_{\omega_{t+1}}$ 
21:  end if
22: end for
```

fixed width d . SAT's communication cost *per round* can be expressed as $\mathcal{O}(MLd^2 + \sum_{m=1}^M |\bigcup_{v \in \mathcal{V}_m} \mathcal{N}(v) \setminus \mathcal{V}_m| Ld + NLd)$, where the first term denotes the cost for pull/push of GNN parameters or gradients, the second term and the third term represent the cost for pull and push of node embeddings, where N is the original graph size. To reduce the accumulated communication and computation cost, we consider decreasing the frequency of finetuning the embedding predictor by a factor every ΔT epoch (Line 17 in Algorithm 1). Such a design for periodic updates of the embedding predictor can greatly reduce the computational and communication overhead by a factor of ΔT .

Experiment

In this section, we evaluate our proposed framework SAT with various experiments. For all distributed experiments, we simulate a distributed training environment using an EC2 g4dn.metal virtual machine (VM) instance on AWS, which has 8 NVIDIA T4 GPUs, 96 vCPUs, and 384 GB main memory. We implemented the shared-memory KVS using the Plasma¹ for embedding storage and retrieval. Detailed experimental settings can be found in the appendix.

Experiment Setting

Datasets. We evaluate SAT with extensive experiments on the node classification task on four large-scale graphs, including Flickr (Zeng et al. 2019), Reddit (Hamilton, Ying,

¹<https://arrow.apache.org/docs/python/plasma.html>

Table 1: Performance comparison (test F1 score) of distributed GNN frameworks. The mean and standard deviation are calculated based on multiple runs with varying seeds. ⁺ denotes the corresponding method combined with our embedding predictor. - denotes not applicable. SAT consistently boosts performance by alleviating the staleness of historical embeddings.

Model	GCN				GAT		
	Flickr	Reddit	ogbn-arxiv	ogbn-products	Flickr	Reddit	ogbn-arxiv
LLCG	50.73±0.15	62.09±0.41	69.80±0.21	76.87±0.32	43.98±0.32	91.10±0.17	68.84±0.22
DistDGL	50.90±0.13	87.02±0.23	69.90±0.17	77.52±0.28	51.50±0.27	92.58±0.12	70.34±0.17
BNS-GCN	51.76±0.21	96.76±0.43	55.49±0.17	78.47±0.31	-	-	-
SANCUS	52.17±0.31	93.81±0.36	70.05±0.25	78.95±0.36	52.29±0.24	93.56±0.23	66.84±0.39
DIGEST	53.78±0.21	95.23±0.43	72.00±0.23	78.56±0.29	52.08±0.21	94.19±0.15	68.35±0.41
DIGEST⁺	53.89±0.19	95.41±0.44	72.13±0.37	79.43±0.31	52.50±0.19	93.94±0.16	68.54±0.32
DIGEST-A	53.10±0.32	94.55±0.37	71.90±0.16	77.36±0.42	52.16±0.17	93.95±0.22	69.04±0.13
DIGEST-A⁺	53.45±0.27	95.25±0.35	72.09±0.21	78.97±0.33	52.36±0.18	94.49±0.26	69.22±0.23
PipeGCN	52.19±0.26	96.97±0.38	53.42±0.19	79.23±0.28	-	-	-
PipeGCN⁺	53.39±0.19	97.02±0.31	55.50±0.24	80.21±0.34	-	-	-

Table 2: Performance comparison (test F1 score) of non-distributed methods. The mean and standard deviation are calculated based on multiple runs with varying seeds. ⁺ denotes the corresponding method combined with our embedding predictor. SAT can also boost the performance of sampling-based methods by reducing the staleness.

Model	GCN				GCN-II		
	Flickr	Reddit	ogbn-arxiv	ogbn-products	Flickr	Reddit	ogbn-arxiv
VR-GCN	48.72±1.23	94.38±1.36	-	-	49.23±0.23	93.57±0.54	-
VR-GCN⁺	49.53±0.75	95.02±0.61	-	-	50.46±0.23	94.36±0.55	-
GNNAutoScale	53.72±0.76	95.34±0.62	71.18±0.97	76.55±0.23	54.19±0.62	96.42±0.56	71.86±1.00
GNNAutoScale⁺	54.03±0.57	96.03±0.56	71.51±1.25	76.83±0.29	54.46±0.21	97.21±0.52	73.28±0.64

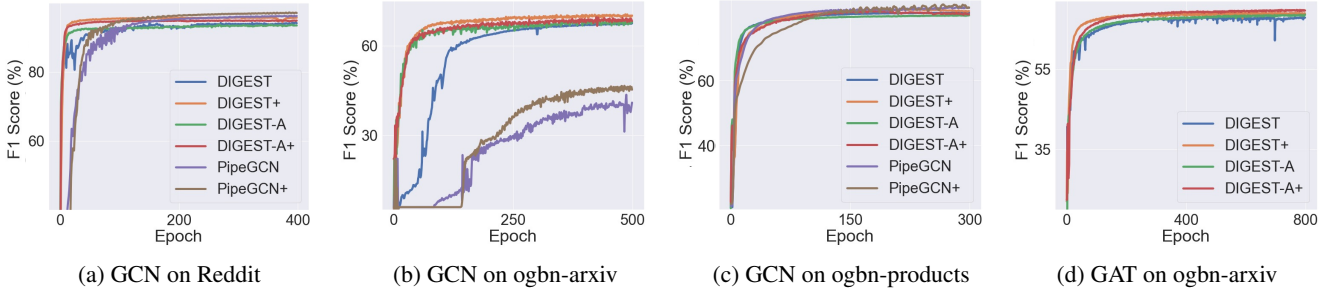


Figure 3: **Performance comparison with and without staleness alleviation by our method.** We report the learning curves of global testing F1 scores for each method. The ⁺ version means having staleness alleviation of our method.

and Leskovec 2017), ogbn-arxiv (Hu et al. 2021), and ogbn-products (Hu et al. 2021). They contain hundreds of thousands to hundreds of millions of nodes. Detailed dataset statistics and descriptions can be found in the appendix.

Comparison Methods. We compare our method with two categories of large-scale GNN methods:

- **Distributed methods:** 1. DistDGL (Zheng et al. 2020), 2. LLCG (Ramezani et al. 2021), 3. DIGEST (Chai et al. 2022), 4. PipeGCN (Wan et al. 2022b), 5. BNS-GCN (Wan et al. 2022a), 6. SANCUS (Peng et al. 2022).
- **Non-distributed methods:** 1. VR-GCN (Chen, Zhu, and Song 2018), 2. GNNAutoScale (Fey et al. 2021).

Performance Evaluation

First, we analyze how our proposed framework can boost the performance of historical-embedding-based methods under the distributed training setting. We evaluate our proposed SAT against four state-of-the-art distributed GNN training methods, including DistDGL, LLCG, DIGEST, and PipeGCN. Since DIGEST and PipeGCN utilize historical embeddings, we implement an upgraded version of DIGEST, DIGEST-A (asynchronous version), and PipeGCN by combining them with our embedding predictor. As shown in Table 1, the upgraded version of DIGEST, DIGEST-A, and PipeGCN achieves better performance compared with their vanilla versions on most datasets, which confirms the effectiveness of our method. LLCG performs worst particularly for the Reddit dataset because in the global server correction of LLCG, only

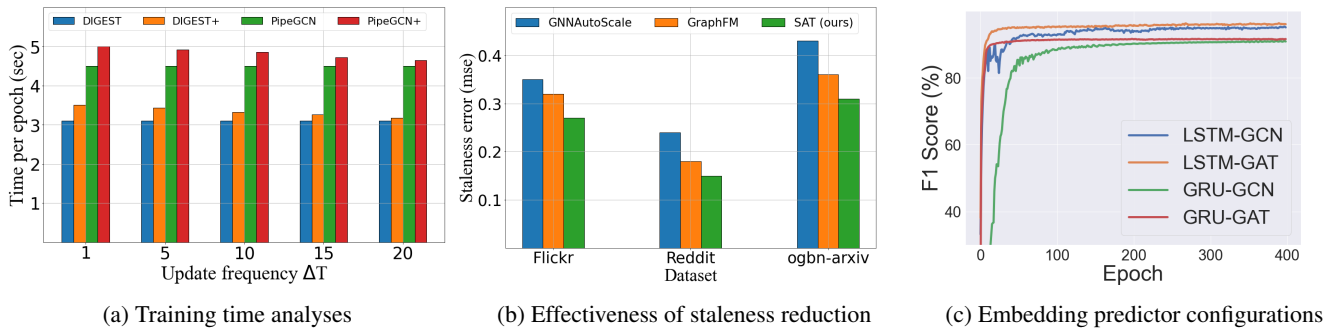


Figure 4: **Left.** The training time induced by our embedding predictor is marginal and can be decreased by increasing the frequency factor ΔT for updating the predictor. **Middle.** SAT can help reduce the staleness by a large margin and is more effective than other staleness reduction methods. **Right.** Comparison of different configurations of the embedding predictor.

Table 3: **GPU memory consumption (GB)** We compare PipeGCN and DIGEST with those combined with our proposed module by including all the information inside a GCN’s receptive field in a single optimization step.

GCN Layers	Method	Flickr	ogbn-arxiv	Reddit
2-layer	PipeGCN	0.23	0.26	0.31
2-layer	PipeGCN+	0.25	0.28	0.34
2-layer	DIGEST	0.18	0.22	0.27
2-layer	DIGEST+	0.20	0.25	0.30
3-layer	PipeGCN	0.26	0.28	0.35
3-layer	PipeGCN+	0.28	0.31	0.37
3-layer	DIGEST	0.20	0.24	0.29
3-layer	DIGEST+	0.23	0.26	0.31

a mini-batch is trained and it is not sufficient to correct the plain GCN. This is also the reason why the authors of LLCG report the performance of a complex model with mixing GCN layers and GraphSAGE layers (Ramezani et al. 2021). DGL achieves good performance on some datasets (e.g., OGB-products) with uniform node sampling strategy and real-time embedding exchanging. However, frequent communication also leads to slow performance increases for dataset Flickr and poor performance for all four datasets. We also provide the learning curve as in Figure 3, where our proposed SAT can consistently improve the performance by some margin for all comparison methods, especially on Reddit with GCN and ogbn-arxiv with GCN.

We further analyze how our proposed framework can boost the performance of historical-embedding-based methods with stochastic training. We pick two widely-used state-of-the-art methods, i.e., VR-GCN and GNNAutoScale, and implement an upgraded version by combining them with SAT. As can be seen in Table 2, both VR-GCN+ and GNNAutoScale+ outperform their counterparts in all cases, confirming the practical effectiveness of our method.

Training Time and Memory Overhead

We further analyze the additional training time induced by our embedding predictor. As shown in Figure 4a, our embedding predictor only introduces marginal additional training time per epoch. More importantly, the training time overhead decreases as the embedding predictor’s update frequency grows, and finally becomes almost neglectable when $\Delta T = 20$. In

practice, we found ΔT between [5, 15] offers an optimal tradeoff between performance and efficiency.

As shown in Table 3, we report the GPU memory consumption by comparing DIGEST/PipeGCN with those combined with our embedding predictor. The comparison results show that in most cases our proposed framework only introduces $< 10\%$ additional GPU memory cost, which largely is attributed to our usage of data compression of historical embeddings. More details of embedding compression and memory cost can be found in the appendix due to space limit.

Measuring the Staleness of Embeddings

As shown in Figure 4b, we visualize and compare the staleness of historical embeddings for three methods, where GNNAutoScale has max staleness while GraphFM (Yu et al. 2022) and our SAT both have mechanisms for staleness reduction. GraphFM is a rule-based approach and is only applicable to GCN. In Figure 4b, SAT consistently achieves the lowest staleness error, indicating the superiority of SAT over GraphFM and the effectiveness of staleness reduction.

Comparison of Different Predictor Configurations

As shown in Figure 4c, GRU-based architectures are consistently outperformed by their LSTM counterpart, possibly due to the weaker capacity of GRU. LSTM-GAT and LSTM-GCN are pretty close in performance, while GCN is more computationally efficient than GAT. In practice, we found LSTM-GCN a go-to choice in most cases due to a better tradeoff between efficiency and performance. Our proposed embedding predictor is general which means more advanced models are also applicable.

Conclusion

Distributed GNN training with historical embeddings is a natural compromise of partition- and propagation-based methods and could enjoy the best of both worlds. However, the embedding staleness could potentially harm the model performance and convergence. In this paper, we present SAT (Staleness-Alleviated Training), a novel and scalable distributed GNN training framework that reduces the embedding staleness in a data-driven manner. We formulate the embedding prediction task as an online prediction problem over the

dynamic embeddings which form a temporal graph. We provide theoretical analyses on the convergence of SAT. Extensive experiments over various comparison methods on multiple real-world graph benchmarks with different GNN operators demonstrate that our proposed SAT can greatly boost the performance of existing historical-embedding-based methods and also achieve faster convergence speed, while the additional cost is marginal.

References

- Angerd, A.; Balasubramanian, K.; and Annavam, M. 2020. Distributed training of graph convolutional networks using subgraph approximation. *arXiv preprint arXiv:2012.04930*.
- Chai, Z.; Bai, G.; Zhao, L.; and Cheng, Y. 2022. Distributed Graph Neural Network Training with Periodic Historical Embedding Synchronization. *arXiv preprint arXiv:2206.00057*.
- Chen, J.; Zhu, J.; and Song, L. 2018. Stochastic Training of Graph Convolutional Networks with Variance Reduction. In *International Conference on Machine Learning*, 942–950. PMLR.
- Chen, M.; Wei, Z.; Huang, Z.; Ding, B.; and Li, Y. 2020. Simple and deep graph convolutional networks. In *International Conference on Machine Learning*, 1725–1735. PMLR.
- Cong, W.; Ramezani, M.; and Mahdavi, M. 2021. On the importance of sampling in learning graph convolutional networks. *arXiv preprint arXiv:2103.02696*.
- Corso, G.; Cavalleri, L.; Beaini, D.; Liò, P.; and Veličković, P. 2020. Principal neighbourhood aggregation for graph nets. *Advances in Neural Information Processing Systems*, 33: 13260–13271.
- Dai, H.; Dai, B.; and Song, L. 2016. Discriminative embeddings of latent variable models for structured data. In *International conference on machine learning*, 2702–2711. PMLR.
- Fey, M.; Lenssen, J. E.; Weichert, F.; and Leskovec, J. 2021. Gnnautoscale: Scalable and expressive graph neural networks via historical embeddings. In *International Conference on Machine Learning*, 3294–3304. PMLR.
- Gu, Z.; Zhang, K.; Bai, G.; Chen, L.; Zhao, L.; and Yang, C. 2023. Dynamic Activation of Clients and Parameters for Federated Learning over Heterogeneous Graphs. ICDE.
- Hamilton, W.; Ying, Z.; and Leskovec, J. 2017. Inductive representation learning on large graphs. *Advances in neural information processing systems*, 30.
- Hu, W.; Fey, M.; Ren, H.; Nakata, M.; Dong, Y.; and Leskovec, J. 2021. Ogb-lsc: A large-scale challenge for machine learning on graphs. *arXiv preprint arXiv:2103.09430*.
- Hu, W.; Fey, M.; Zitnik, M.; Dong, Y.; Ren, H.; Liu, B.; Catasta, M.; and Leskovec, J. 2020. Open graph benchmark: Datasets for machine learning on graphs. *Advances in neural information processing systems*, 33: 22118–22133.
- Huo, Z.; Gu, B.; Huang, H.; et al. 2018. Decoupled parallel backpropagation with convergence guarantee. In *International Conference on Machine Learning*, 2098–2106. PMLR.
- Jia, Z.; Lin, S.; Gao, M.; Zaharia, M.; and Aiken, A. 2020. Improving the accuracy, scalability, and performance of graph neural networks with roc. *Proceedings of Machine Learning and Systems*, 2: 187–198.
- Kipf, T. N.; and Welling, M. 2016. Semi-supervised classification with graph convolutional networks. *arXiv preprint arXiv:1609.02907*.
- Lei, K.; Qin, M.; Bai, B.; Zhang, G.; and Yang, M. 2019. GCN-GAN: A non-linear temporal link prediction model for weighted dynamic networks. In *IEEE INFOCOM 2019-IEEE Conference on Computer Communications*, 388–396. IEEE.
- Ling, C.; Jiang, J.; Wang, J.; and Liang, Z. 2022. Source localization of graph diffusion via variational autoencoders for graph inverse problems. In *Proceedings of the 28th ACM SIGKDD conference on knowledge discovery and data mining*, 1010–1020.
- Ling, C.; Jiang, J.; Wang, J.; Thai, M. T.; Xue, R.; Song, J.; Qiu, M.; and Zhao, L. 2023. Deep graph representation learning and optimization for influence maximization. In *International Conference on Machine Learning*, 21350–21361. PMLR.
- Ma, L.; Yang, Z.; Miao, Y.; Xue, J.; Wu, M.; Zhou, L.; and Dai, Y. 2019. {NeuGraph}: Parallel Deep Neural Network Computation on Large Graphs. In *2019 USENIX Annual Technical Conference (USENIX ATC 19)*, 443–458.
- Peng, J.; Chen, Z.; Shao, Y.; Shen, Y.; Chen, L.; and Cao, J. 2022. Sancus: stateless-aware communication-avoiding full-graph decentralized training in large-scale graph neural networks. *Proceedings of the VLDB Endowment*, 15(9): 1937–1950.
- Ramezani, M.; Cong, W.; Mahdavi, M.; Kandemir, M. T.; and Sivasubramanian, A. 2021. Learn Locally, Correct Globally: A Distributed Algorithm for Training Graph Neural Networks. *arXiv preprint arXiv:2111.08202*.
- Sen, P.; Namata, G.; Bilgic, M.; Getoor, L.; Galligher, B.; and Eliassi-Rad, T. 2008. Collective classification in network data. *AI magazine*, 29(3): 93–93.
- Thorpe, J.; Qiao, Y.; Eyolfson, J.; Teng, S.; Hu, G.; Jia, Z.; Wei, J.; Vora, K.; Netravali, R.; Kim, M.; and Xu, G. H. 2021. Dorylus: Affordable, Scalable, and Accurate GNN Training with Distributed CPU Servers and Serverless Threads. In *15th USENIX Symposium on Operating Systems Design and Implementation (OSDI 21)*, 495–514. USENIX Association. ISBN 978-1-939133-22-9.
- Tripathy, A.; Yelick, K.; and Buluç, A. 2020. Reducing communication in graph neural network training. In *SC20: International Conference for High Performance Computing, Networking, Storage and Analysis*, 1–14. IEEE.
- Veličković, P.; Cucurull, G.; Casanova, A.; Romero, A.; Lio, P.; and Bengio, Y. 2017. Graph attention networks. *arXiv preprint arXiv:1710.10903*.
- Wan, C.; Li, Y.; Li, A.; Kim, N. S.; and Lin, Y. 2022a. BNS-GCN: Efficient full-graph training of graph convolutional networks with partition-parallelism and random boundary node sampling. *Proceedings of Machine Learning and Systems*, 4: 673–693.
- Wan, C.; Li, Y.; Wolfe, C. R.; Kyrillidis, A.; Kim, N. S.; and Lin, Y. 2022b. PipeGCN: Efficient full-graph training of

graph convolutional networks with pipelined feature communication. *arXiv preprint arXiv:2203.10428*.

Wu, L.; Cui, P.; Pei, J.; Zhao, L.; and Song, L. 2022. Graph neural networks. In *Graph Neural Networks: Foundations, Frontiers, and Applications*, 27–37. Springer.

Xu, A.; Huo, Z.; and Huang, H. 2020. On the acceleration of deep learning model parallelism with staleness. In *Proceedings of the IEEE/CVF Conference on Computer Vision and Pattern Recognition*, 2088–2097.

Ying, R.; He, R.; Chen, K.; Eksombatchai, P.; Hamilton, W. L.; and Leskovec, J. 2018. Graph convolutional neural networks for web-scale recommender systems. In *Proceedings of the 24th ACM SIGKDD international conference on knowledge discovery & data mining*, 974–983.

Yu, H.; Wang, L.; Wang, B.; Liu, M.; Yang, T.; and Ji, S. 2022. GraphFM: Improving large-scale GNN training via feature momentum. In *International Conference on Machine Learning*, 25684–25701. PMLR.

Zeng, H.; Zhou, H.; Srivastava, A.; Kannan, R.; and Prasanna, V. 2019. Graphsaint: Graph sampling based inductive learning method. *arXiv preprint arXiv:1907.04931*.

Zhang, Y.; and Yang, Q. 2021. A survey on multi-task learning. *IEEE Transactions on Knowledge and Data Engineering*, 34(12): 5586–5609.

Zheng, D.; Ma, C.; Wang, M.; Zhou, J.; Su, Q.; Song, X.; Gan, Q.; Zhang, Z.; and Karypis, G. 2020. Distdgl: distributed graph neural network training for billion-scale graphs. In *2020 IEEE/ACM 10th Workshop on Irregular Applications: Architectures and Algorithms (IA3)*, 36–44. IEEE.

Zhu, R.; Zhao, K.; Yang, H.; Lin, W.; Zhou, C.; Ai, B.; Li, Y.; and Zhou, J. 2019. Aligraph: a comprehensive graph neural network platform. *arXiv preprint arXiv:1902.08730*.

Appendix

In this appendix, we describe the detailed experimental setup, additional experimental results, complete proofs, our limitations, etc. Our source code for the preprint version can be found here: <https://anonymous.4open.science/r/SAT-CA0C>. Please note that the code is subjected to reorganization to improve readability.

Experimental Setting Details

All the experiments are done on an EC2 `g4dn.metal` virtual machine (VM) instance on AWS, which has 8 NVIDIA T4 GPUs, 96 vCPUs, and 384 GB main memory. Other important information including operation system version, Linux kernel version, and CUDA version is summarized in Table 4. For a fair comparison, we use the same optimizer (Adam), learning rate, and graph partition algorithm for all the frameworks, PipeGCN, PipeGCN⁺, GNNAutoscale, GNNAutoscale⁺, DIGEST, DIGEST⁺, VR-GCN, VR-GCN⁺, DIGEST-A and DIGEST-A⁺, and GraphFM. For parameters that are unique to PipeGCN, GNNAutoscale, DIGEST, VR-GCN, and DIGEST-A, such as the number of neighbors sampled from each layer for each node and the number of layers, we choose the same value for PipeGCN⁺, GNNAutoscale⁺, DIGEST⁺, VR-GCN⁺ and DIGEST-A⁺. Each of the ten frameworks has a set of parameters that are exclusively unique to that framework; for these exclusive parameters, we tune them in order to achieve the best performance. Please refer to the configuration files under `small_benchmark/conf` for detailed configuration setups for all the models and datasets.

We use eight datasets: Cora (Sen et al. 2008; Ling et al. 2023), Citeseer (Sen et al. 2008), Pubmed (Sen et al. 2008), OGB-Arxiv (Hu et al. 2020), Flickr (Zeng et al. 2019), Reddit (Zeng et al. 2019), OGB-Products (Hu et al. 2020), and OGB-Papers100M (Hu et al. 2021) for evaluation. The detailed information of these datasets is summarized in Table 5.

Dataset Details

We expand upon the datasets used for our experiments in this section.

- **Cora:** The dataset consists of 2,708 research papers from computer science, categorized into seven classes. Each paper is represented by a bag-of-words feature vector, indicating word occurrences. The dataset also includes citation links between papers, forming a citation graph.
- **Citeseer:** The CiteSeer dataset, also known as the CiteSeer digital library, is a collection of scientific research papers primarily focused on computer science and related fields. It was developed to facilitate information retrieval and citation analysis in the academic community. One notable feature of the CiteSeer dataset is its citation network, which represents the relationships between papers based on citations.
- **Pubmed:** This dataset refers to a collection of scientific articles and related metadata available through the PubMed database. The dataset provides structured information about

articles, including titles, abstracts, authors, affiliations, publication dates, and often keywords or MeSH terms (Medical Subject Headings) that categorize the content.

- **Flickr:** Flickr is a popular online photo-sharing platform where users can upload, share, and explore a wide range of images. Flickr dataset is a collection of images and associated metadata obtained from the Flickr platform, containing descriptions and common properties of images.
- **Reddit:** This is a collection of data extracted from the social media platform Reddit, which is a popular online community where users can participate in discussions, share content, and engage with a wide range of topics. The dataset often includes information such as the text of the posts and comments, timestamps, user IDs, upvotes or downvotes, subreddit affiliations, and other relevant attributes. These attributes provide valuable insights into user behavior, community dynamics, and the content shared on the platform.
- **OGB-Arxiv:** OGB-Arxiv, short for Open Graph Benchmark Arxiv, is a dataset specifically designed for graph machine learning tasks. It is part of the Open Graph Benchmark (OGB) project (Hu et al. 2021), which aims to provide standardized and accessible benchmarks for evaluating graph-based machine learning algorithms. It focuses on academic papers from the Arxiv preprint server, covering a wide range of research areas such as computer science, physics, mathematics, and more. The dataset consists of a large collection of papers, where each paper is represented as a node in a citation graph. The citation graph captures the citation relationships between papers, allowing researchers to analyze the structure of academic literature and evaluate graph-based algorithms.
- **OGB-Products:** OGB-Products, part of the Open Graph Benchmark (OGB) project (Hu et al. 2021), is a dataset designed for graph-based machine learning tasks in the context of e-commerce and product recommendation systems. It aims to provide a standardized benchmark to evaluate algorithms for product-related graph analysis. This dataset consists of a large-scale product graph that represents relationships between products. Each product is represented as a node in the graph, and the edges capture different types of relationships, such as co-purchase, co-rating, or similarity between products. The dataset also includes various attributes associated with the products, such as titles, descriptions, categories, and prices.

Details of Comparison Methods

- **Single-machine Sampling-based GNN Training Baseline.** 1). *GNNAutoscale (GAS)* (Fey et al. 2021): This is a scalable framework that dynamically adjusts the scale and complexity of neural networks to optimize performance and resource utilization. 2). *VR-GCN* (Chen, Zhu, and Song 2018): This is a framework that is trained stochastically and reduces the variance to a significant magnitude.
- **Distributed GNN Training Baseline.** 1). *LLCG* (Ramezani et al. 2021): This framework accelerates the sampling method under the memory budget. 2). *DistDGL* (Zheng et al. 2020): It is the system to help

Table 4: Summary of the environmental setup of our testbed.

OS	Linux kernel	CUDA	Driver	PyTorch	PyTorch Geometric	PyTorch Sparse
Ubuntu 20.04	5.15.0	11.6	510.73.08	1.12.1	2.2.0	0.6.16

Table 5: Summary of dataset statistics.

Dataset	# Nodes	# Edges	# Features	# Classes
Cora	2,708	10,556	1,433	7
Citeseer	3,327	9,104	3,703	6
Pubmed	19,717	88,648	500	3
Flickr	89,250	899,756	500	7
Reddit	232,965	23,213,838	602	41
OGB-Arxiv	169,343	2,315,598	128	40
OGB-Products	2,449,029	123,718,280	100	47
OGB-Papers100M	111,059,956	1,615,685,872	128	172

train large graphs with millions of nodes and billions of edges based on DGL. 3). *DIGEST* (Chai et al. 2022): This is a framework that extends GNNAutoscale in a distributed synchronous manner. 4). *DIGEST-A* (Chai et al. 2022): This is a framework that extends GNNAutoscale in a distributed asynchronous manner with the help of Plasma. 5). *PipeGCN* (Wan et al. 2022b): This is a framework that makes the training of large graphs more efficient through pipelined feature communication.

Parameter Setting

We use Adam optimizer for all our experiments and the learning rate of all embedding predictors is set to be $1e-1$. The hyperparameters of base models are following those in the original paper. For example, the configuration of the base model for DIGEST⁺ is the same as the configuration of DIGEST. We set hyperparameters for each comparison method with respect to the recommendation in their original paper, and we specify the architecture as well as other details for each dataset’s experiments as follows.

- **Cora.** The number of layers and cells of the embedding predictor is set to be 2, and the hidden dimension is 16. We use the ReLU layer after each hidden layer. The frequency of the training of the embedding predictor is set to be 10 to ensure a better performance.
- **Citeseer** The number of layers and cells of the embedding predictor are set to be 1 and 3 respectively. We use the ReLU layer after each hidden layer. The frequency of the embedding predictor training is 8.
- **Pubmed** The number of layers and cells of the embedding predictor are set to be 2. We use the ReLU layer after each hidden layer. The frequency of the embedding predictor training is 10.
- **Flickr.** The number of layers and cells of the embedding predictor is set to be 2. We use the ReLU layer after each hidden layer. The frequency of the embedding predictor training is 15.
- **Reddit.** The number of layers and cells of the embedding predictor is set to be 3. We use the ReLU layer after each

hidden layer. The frequency of the embedding predictor training is 10.

- **OGB-Arxiv.** The number of layers and cells of the embedding predictor is set to be 3 and 2 respectively. We use the ReLU layer after each hidden layer. The frequency of the embedding predictor training is 15.
- **OGB-Products.** The number of layers and cells of the embedding predictor is set to be 3. We use the ReLU layer after each hidden layer. The frequency of the embedding predictor training is 15.

Limitations

In this section, we discuss some potential limitations of our work. First, just like most existing work in distributed GNN training, our goal is to find a better trade-off between embedding approximation quality and communication cost. In this work, the proposed embedding predictor aims at improving the embedding approximation quality, while the communication cost is the same as the baseline method (e.g., DIGEST, PipeGCN). Notice that our embedding predictor does NOT introduce additional communication costs. Hence, how to reduce the communication cost of existing distributed GNN work is beyond our scope but is for sure a very important and promising research direction. Second, how to optimize the nested loss function of SAT (Eq. 9) is not fixed but applicable to various approaches. In this paper, we choose to optimize it alternatively, i.e., optimize one variable while keeping the others fixed, due to its simplicity and practical effectiveness. However, we believe more advanced approaches are also worth exploring. In addition, there is a recent research interest in federated learning on non-i.i.d data such as graphs (Gu et al. 2023). Our current method does not consider privacy issues, but we believe our idea has the potential to be extended to the federated learning setting to help reduce the staleness.

Data Compression for Historical Embedding Storage

In SAT, our embedding predictor aims to reduce the staleness of historical embeddings based on the induced temporal

graph, by optimizing the following loss function

$$\min_{\omega_t} \frac{1}{M} \sum_{m=1}^M \left\| \mathbf{g}_{\omega_t}(\{\bar{\mathcal{G}}_m^{(s)}\}_{t-\tau \leq s \leq t-1}) - \mathbf{H}^{(t,m)} \right\|, \\ \text{s.t., } \delta \hat{\mathbf{H}}^{(t,m)} < \delta \mathbf{H}^{(t-1,m)}. \quad (15)$$

Although we introduce the hyperparameter τ as the length of the *sliding window* to obtain a constant memory complexity with respect to t , the memory cost of the temporal graph can still be prohibitive when the original graph is huge. To this end, we borrow the idea of data compression to reduce the cost of storage for historical embeddings.

In this work, we design a simple yet effective compression scheme based on the *Encoded Polyline Algorithm*² (or polyline encoding.) Polyline encoding is a lossy compression algorithm that converts a rounded binary value into a series of character codes for ASCII characters using the base64 encoding scheme. It can be configured to maintain a configurable precision by rounding the value to a specified decimal place. With the appropriate precision, the model could achieve the largest communication saving and minor performance loss. We empirically found that, by choosing proper parameters for the compression algorithm, we can achieve up to **3.5**× of compression ratio for the historical embeddings. Hence, although historical embeddings of more than 1 epoch are stored, the overall memory cost of SAT is still comparable to the baselines (please refer to Table 2 of our main text.)

As a byproduct, the compression algorithm can also help reduce the communication cost of SAT. To see this, the pull and push operations as shown in our Algorithm 1 (main text) can both enjoy a reduced communication cost if we compress the node embeddings by using the polyline encoding before triggering the pull/push operations. After the communication, we can decompress the embeddings and follow the procedures as defined in SAT.

Additional Results

Comparison over More GNN Operators In this section, we investigate the impact of different GNN operators, including GCN (Hamilton, Ying, and Leskovec 2017), GAT (Veličković et al. 2017), GCN-2 (Chen et al. 2020), and PNA (Corso et al. 2020). We test each GNN operator by using them as the backbone GNN and implement them as DIGEST⁺. The performance is shown in the following table:

Table 6: Comparison of different GNN operators.

GNN Operator	Flickr	obgn-arxiv	Reddit
GCN	53.89 ± 0.19	72.13 ± 0.17	95.41 ± 0.44
GAT	52.50 ± 0.16	68.54 ± 0.32	93.94 ± 0.16
GCN-2	54.03 ± 0.32	72.79 ± 0.39	95.22 ± 0.27
PNA	54.17 ± 0.25	71.93 ± 0.31	95.49 ± 0.33

As can be seen in Table 6, our framework can enhance the performance of various GNN operators.

²<https://developers.google.com/maps/documentation/utilities/polylinealgorithm>

Comparison of different RNN-GNN Architectures As can be seen, on both datasets LSTM-GCN achieves the best performance among the three architectures. GRU-based architectures seem to be consistently outperformed by their LSTM counterpart, possibly due to the weaker capacity of GRU. LSTM-GAT and LSTM-GCN are pretty close in both figures, while GCN is more computationally efficient.

Theoretical Proof

In this section, we provide the formal proof for all the theories presented in the main paper.

Proof of Theorem 4.1 In this section, we prove the convergence of SAT. First, we introduce some notions, definitions, and necessary assumptions.

Preliminaries. We consider GCN in our proof without loss of generality. We denote the input graph as $\mathcal{G} = (\mathcal{V}, \mathcal{E})$, L -layer GNN as f , feature matrix as X , weight matrix as W . The forward propagation of one layer of GCN is

$$Z^{(\ell+1)} = PH^{(\ell)}W^{(\ell)}, \quad H^{(\ell+1)} = \sigma(Z^{(\ell)}) \quad (16)$$

where ℓ is the layer index, σ is the activation function, and P is the propagation matrix following the definition of GCN (Kipf and Welling 2016). Notice $H^{(0)} = X$. We can further define the $(\ell + 1)$ -th layer of GCN as:

$$f^{(\ell+1)}(H^{(\ell)}, W^{(\ell)}) := \sigma(PH^{(\ell)}W^{(\ell)}) \quad (17)$$

The backward propagation of GCN can be expressed as follow:

$$G_H^{(\ell)} = \nabla_H f^{(\ell+1)}(H^{(\ell)}, W^{(\ell)}, G_H^{(\ell+1)}) \\ := P^\top D^{(\ell+1)}(W^{(\ell+1)})^\top \quad (18)$$

$$G_W^{(\ell+1)} = \nabla_W f^{(\ell+1)}(H^{(\ell+1)}, W^{(\ell)}, G_H^{(\ell+1)}) \\ := (PH^{(\ell)})^\top D^{(\ell+1)} \quad (19)$$

where

$$D^{(\ell+1)} = G_H^{(\ell)} \circ \sigma'(PH^{(\ell)}W^{(\ell+1)}) \quad (20)$$

and \circ represents the Hadamard product.

Under a distributed training setting, for each subgraph $\mathcal{G}_m = (\mathcal{V}_m, \mathcal{E}_m)$, $m = 1, 2, \dots, M$, the propagation matrix can be decomposed into two independent matrices, i.e. $P = P_{m,in} + P_{m,out}$, where $P_{m,in}$ denotes the propagation matrix for nodes inside the subgraph \mathcal{G}_m while $P_{m,out}$ denotes that for neighbor nodes outside \mathcal{G}_m . If it will not cause confusion, we will use P_{in} and P_{out} in our future proof for simpler notation.

For SAT, the forward propagation of a single layer of GCN can be expressed as

$$\tilde{Z}_m^{(t,\ell+1)} = P_{in} \tilde{H}_m^{(t,\ell)} \tilde{W}_m^{(t,\ell)} + P_{out} \tilde{H}_m^{(t-1,\ell)} \tilde{W}_m^{(t,\ell)} \\ \tilde{H}_m^{(t,\ell+1)} = \sigma(\tilde{Z}_m^{(t,\ell)}) \quad (21)$$

where we use \tilde{H} to differentiate with the counterpart without staleness, i.e., H (same for other variables). t is the training iteration index. Similarly, we can define each layer as a single function

$$\tilde{f}_m^{(t,\ell+1)}(\tilde{H}_m^{(t,\ell)}, \tilde{W}_m^{(t,\ell)}) \\ := \sigma(P_{in} \tilde{H}_m^{(t,\ell)} \tilde{W}_m^{(t,\ell)} + P_{out} \tilde{H}_m^{(t-1,\ell)} \tilde{W}_m^{(t,\ell)}) \quad (22)$$

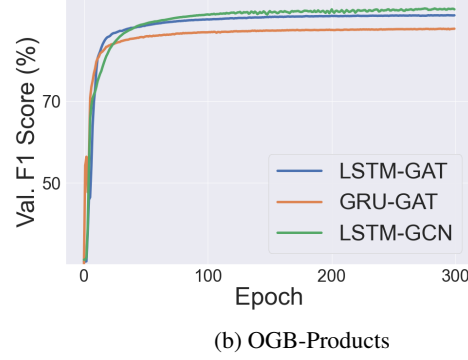
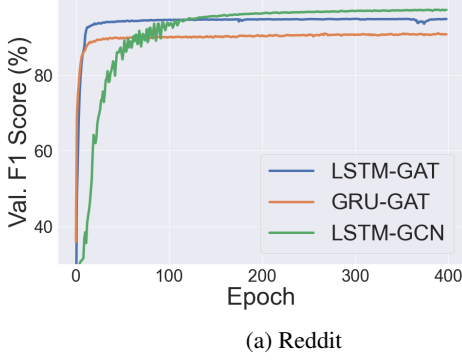


Figure 5: Performance comparison of different architectures of RNN-GNN.

Note that $\tilde{H}_m^{(t-1, \ell-1)}$ is not part of the input since it is the stale results from the previous iteration, i.e., it can be regarded as a constant in the current iteration.

Now we can give the definition of back-propagation in SAT:

$$\begin{aligned} \tilde{G}_{H,m}^{(t,\ell)} &= \nabla_H \tilde{f}_m^{(t,\ell+1)}(\tilde{H}_m^{(\ell)}, \tilde{W}_m^{(\ell)}, \tilde{G}_{H,m}^{(\ell+1)}) \\ &:= P_{in}^\top \tilde{D}_m^{(t,\ell+1)} (\tilde{W}_m^{(t,\ell+1)})^\top \\ &\quad + P_{out}^\top \tilde{D}_m^{(t-1,\ell+1)} (\tilde{W}_m^{(t,\ell+1)})^\top \end{aligned} \quad (23)$$

$$\begin{aligned} \tilde{G}_{W,m}^{(t,\ell+1)} &= \nabla_W \tilde{f}_m^{(t,\ell+1)}(\tilde{H}_m^{(t,\ell+1)}, \tilde{W}_m^{(t,\ell)}, \tilde{G}_{H,m}^{(t,\ell+1)}) \\ &:= (P_{in} \tilde{H}_m^{(t,\ell)} + P_{out} \tilde{H}_m^{(t-1,\ell-1)})^\top \tilde{D}_m^{(t,\ell+1)} \end{aligned} \quad (24)$$

where

$$\begin{aligned} \tilde{D}_m^{(t,\ell+1)} &= G_{H,m}^{(\ell)} \circ \sigma'(P_{in} \tilde{H}_m^{(t,\ell)} \tilde{W}_m^{(t,\ell)} \\ &\quad + P_{out} \tilde{H}_m^{(t-1,\ell-1)} \tilde{W}_m^{(t,\ell)}) \end{aligned} \quad (25)$$

In our proof, we use $\mathcal{L}(W^{(t)})$ to denote the global loss with GCN parameter W after t iterations, and use $\tilde{\mathcal{L}}_m(W_m^{(t)})$ to denote the local loss for the m -th subgraph with model parameter $W_m^{(t)}$ after t iterations computed by SAT.

Assumptions. Here we introduce some assumptions about the GCN model and the original input graph. These assumptions are standard ones that are also used in (Chen, Zhu, and Song 2018; Cong, Ramezani, and Mahdavi 2021; Wan et al. 2022b).

Assumption 0.2. The loss function $Loss(\cdot, \cdot)$ is C_{Loss} -Lipchitz continuous and L_{Loss} -Lipschitz smooth with respect to the last layer’s node representation, i.e.,

$$\begin{aligned} |Loss(\mathbf{h}_v^{(L)}, \mathbf{y}_v) - Loss(\mathbf{h}_w^{(L)}, \mathbf{y}_v)| \\ \leq C_{Loss} \|\mathbf{h}_v^{(L)} - \mathbf{h}_w^{(L)}\|_2 \end{aligned} \quad (26)$$

and

$$\begin{aligned} \|\nabla Loss(\mathbf{h}_v^{(L)}, \mathbf{y}_v) - \nabla Loss(\mathbf{h}_w^{(L)}, \mathbf{y}_v)\|_2 \\ \leq L_{Loss} \|\mathbf{h}_v^{(L)} - \mathbf{h}_w^{(L)}\|_2 \end{aligned} \quad (27)$$

Assumption 0.3. The activation function $\sigma(\cdot)$ is C_σ -Lipchitz continuous and L_σ -Lipschitz smooth, i.e.

$$\|\sigma(Z_1^{(\ell)}) - \sigma(Z_2^{(\ell)})\|_2 \leq C_\sigma \|Z_1^{(\ell)} - Z_2^{(\ell)}\|_2 \quad (28)$$

and

$$\|\sigma'(Z_1^{(\ell)}) - \sigma'(Z_2^{(\ell)})\|_2 \leq L_\sigma \|Z_1^{(\ell)} - Z_2^{(\ell)}\|_2 \quad (29)$$

Assumption 0.4. $\forall \ell$ that $\ell = 1, 2, \dots, L$, we have

$$\|W^{(\ell)}\|_F \leq K_W, \|P^{(\ell)}\|_P \leq K_W, \|X^{(\ell)}\|_F \leq K_X. \quad (30)$$

Assumption 0.5. Let $\hat{H}_m^{(t,\ell+1)}$ be the historical embedding before being corrected by the embedding predictor. The staleness satisfies the non-increasing property:

$$\|\tilde{H}_m^{(t,\ell+1)} - H_m^{(t,\ell+1)}\| \leq \|\hat{H}_m^{(t,\ell+1)} - H_m^{(t,\ell+1)}\| \quad (31)$$

Now we can introduce the proof of our Theorem 4.1. We consider a GCN with L layers that is L_f -Lipschitz smooth, i.e., $\|\nabla \mathcal{L}(W_1) - \nabla \mathcal{L}(W_2)\|_2 \leq L_f \|W_1 - W_2\|_2$.

Theorem 0.6 (Formal version of Theorem 4.1). *There exists a constant E such that for any arbitrarily small constant $\epsilon > 0$, we can choose a learning rate $\eta = \frac{\sqrt{M}\epsilon}{E}$ and number of training iterations $T = (\mathcal{L}(W^{(1)}) - \mathcal{L}(W^*)) \frac{E}{\sqrt{M}} \epsilon^{-\frac{3}{2}}$, such that*

$$\frac{1}{T} \sum_{t=1}^T \|\nabla \mathcal{L}(W^{(t)})\|^2 \leq \mathcal{O}\left(\frac{1}{T^{\frac{2}{3}} M^{\frac{1}{3}}}\right) \quad (32)$$

where $W^{(t)}$ and W^* denotes the parameters at iteration t and the optimal one, respectively.

Proof. Beginning from the assumption of smoothness of loss function,

$$\begin{aligned} \mathcal{L}(W^{t+1}) &\leq \mathcal{L}(W^t) + \langle \nabla \mathcal{L}(W^t), W^{t+1} - W^{(t)} \rangle \\ &\quad + \frac{L_f}{2} \|W^{t+1} - W^{(t)}\|_2^2 \end{aligned} \quad (33)$$

Recall that the update rule of SAT is

$$W^{(t+1)} = W^{(t)} - \frac{\eta}{M} \sum_{m=1}^M \nabla \tilde{\mathcal{L}}_m(W_m^{(t)}) \quad (34)$$

so we have

$$\begin{aligned}
& \mathcal{L}(W^t) + \left\langle \nabla \mathcal{L}(W^t), W^{(t+1)} - W^{(t)} \right\rangle \\
& + \frac{L_f}{2} \|W^{(t+1)} - W^{(t)}\|_2^2 \\
& = \mathcal{L}(W^t) - \eta \left\langle \nabla \mathcal{L}(W^t), \frac{1}{M} \sum_{m=1}^M \nabla \tilde{\mathcal{L}}_m(W_m^{(t)}) \right\rangle \quad (35) \\
& + \frac{\eta^2 L_f}{2} \left\| \frac{1}{M} \sum_{m=1}^M \nabla \tilde{\mathcal{L}}_m(W_m^{(t)}) \right\|_2^2
\end{aligned}$$

Denote $\delta_m^{(t)} = \nabla \tilde{\mathcal{L}}_m(W_m^{(t)}) - \nabla \mathcal{L}_m(W_m^{(t)})$, we have

$$\begin{aligned}
\mathcal{L}(W^{t+1}) & \leq \mathcal{L}(W^t) - \\
& \eta \left\langle \nabla \mathcal{L}(W^t), \frac{1}{M} \sum_{m=1}^M \left(\nabla \mathcal{L}_m(W_m^{(t)}) + \delta_m^{(t)} \right) \right\rangle \\
& + \frac{\eta^2 L_f}{2} \left\| \frac{1}{M} \sum_{m=1}^M \left(\nabla \mathcal{L}_m(W_m^{(t)}) + \delta_m^{(t)} \right) \right\|_2^2 \quad (36)
\end{aligned}$$

Without loss of generality, assume the original graph can be divided evenly into M subgraphs and denote $N = |\mathcal{V}|$ as the original graph size, i.e., $N = M \cdot S$, where S is each subgraph size. Notice that

$$\begin{aligned}
\nabla \mathcal{L}(W^t) & = \frac{1}{N} \sum_{i=1}^N \nabla \text{Loss}(f_i^{(L)}, y_i) \\
& = \frac{1}{M} \left\{ \sum_{m=1}^M \frac{1}{S} \sum_{i=1}^S \nabla \text{Loss}(f_{m,i}^{(L)}, y_{m,i}) \right\} \quad (37)
\end{aligned}$$

which is essentially

$$\nabla \mathcal{L}(W^t) = \frac{1}{M} \sum_{m=1}^M \nabla \mathcal{L}_m(W_m^{(t)}) \quad (38)$$

Plugging the equation above into Eq. 36, we have

$$\mathcal{L}(W^{t+1}) \leq \mathcal{L}(W^t) - \frac{\eta}{2} \|\nabla \mathcal{L}(W^t)\|_2^2 + \frac{\eta^2 L_f}{2} \left\| \frac{1}{M} \sum_{m=1}^M \delta_m^{(t)} \right\|_2^2 \quad (39)$$

which after rearranging the terms leads to

$$\|\nabla \mathcal{L}(W^t)\|_2^2 \leq \frac{2}{\eta} (\mathcal{L}(W^t) - \mathcal{L}(W^{t+1})) + \eta L_f \left\| \frac{1}{M} \sum_{m=1}^M \delta_m^{(t)} \right\|_2^2 \quad (40)$$

By taking $\eta < 1/L_f$, using the four assumptions defined earlier and Corollary A.10 in (Wan et al. 2022b), and summing up the inequality above over all iterations, i.e., $t = 1, 2, \dots, T$, we have

$$\begin{aligned}
\frac{1}{T} \sum_{t=1}^T \|\nabla \mathcal{L}(W^{(t)})\|_2^2 & \leq \frac{2}{\eta T} (\mathcal{L}(W^1) - \mathcal{L}(W^{T+1})) + \frac{\eta^2 E^2}{M} \\
& \leq \frac{2}{\eta T} (\mathcal{L}(W^1) - \mathcal{L}(W^*)) + \frac{\eta^2 E^2}{M} \quad (41)
\end{aligned}$$

where W^* denotes the minima of the loss function and E is a constant depends on E' .

Finally, taking $\eta = \frac{\sqrt{M}\epsilon}{E}$ and $T = (\mathcal{L}(W^{(1)}) - \mathcal{L}(W^*)) \frac{E}{\sqrt{M}} \epsilon^{-\frac{3}{2}}$ finishes the proof. \square